Strong magnetoelastic effect in CeCo$_{1-x}$Fe$_x$Si as Néel order is suppressed

V. F. Correa , A. G. Villagrán Asiares,[*] D. Betancourth, S. Encina, P. Pedrazzini, P. S. Cornaglia, D. J. García, and J. G. Sereni
Centro Atómico Bariloche (CNEA) and Instituto Balseiro (U. N. Cuyo), 8400 Bariloche, Río Negro, Argentina

B. Maiorov
National High Magnetic Field Laboratory, MS E536 Los Alamos National Laboratory, Los Alamos, New Mexico 87545, USA

N. Caroca Canales and C. Geibel
Max-Planck-Institut für Chemische Physik fester Stoffe, D-01187 Dresde, Germany

A very strong magnetoelastic effect in the CeCo$_{1-x}$Fe$_x$Si alloys is reported. The strength of the magnetostrictive effect can be tuned upon changing x. The moderate low-temperature linear magnetostriction observed at low Fe concentrations becomes very large ($\frac{\Delta L}{L}(16T, 2K) = 3 \times 10^{-3}$) around the critical concentration $x_c \approx 0.23$ at which the long-range antiferromagnetic order vanishes. Upon increasing doping through the nonmagnetic region ($x > x_c$), the magnetostriction strength gradually weakens again. The interplay between magnetic order and the Kondo screening appears to cause an enhanced valence susceptibility slightly changing the Ce ions valence, ultimately triggering the large magnetostriction observed around the critical concentration. Previous studies of the evolution of the lattice parameters with x as well as magnetization and x-ray absorption spectroscopy measurements support this hypothesis.

I. INTRODUCTION

Magnetic order has been traditionally discussed and described in terms of effective interactions between either localized and/or itinerant electrons [1]. Even though the effective coupling can have a substantial and nontrivial dependence on the distance or effective path between magnetic moments (as in the RKKY mechanism), the lattice effects have often been regarded as a second-order property concomitant to the magnetic order, but not decisive to it [2]. In other words, magnetic ground state is first solved supposing a nondeformable lattice. Strains may be then incorporated but they usually do not modify the magnetic state. The reason for this is that solids are typically hard and compact enough as to prevent any major magnetoelastic effect.

Over the past decades, it has become clear that there are several exceptions to this rule. The most notable is found in magnetic systems with first-order transitions to an ordered state. This turns out to be the signature that the magnetic transition occurs concurrently with an important lattice distortion. A strong volume dependence of the exchange couplings is the main responsible for the effect. Though the key role at such transitions is often played by the magnetic interactions (not by the atomic lattice), it remains true that if there were no spin-lattice coupling the transition would occur at a different temperature or it could lose its first-order nature [2]. Prerequisites for the occurrence of the first-order magnetoelastic transitions

are a strong pressure dependence of the ordering temperature and/or a small bulk modulus [2]. Among pure elements, a good example can be found in the pressure-induced first-order transition from the ferromagnetic α phase to the nonmagnetic ϵ phase of iron [3].

Very large magnetic field-induced strains ($\frac{\Delta L}{L} \geqslant 10^{-3}$) have been observed in different systems such as manganites, magnetic Heusler alloys and diverse transition/rare-earth intermetallic alloys. In manganites, though the observed colossal magnetoresistance (CMR) around the magnetic order transition can be explained without invoking atomic lattice strain, it remains true that whenever there is CMR, there is also a giant magnetostrictive effect [4]. In this case, the strong coupling is not only associated with a strain dependence of the superexchange interaction [5] but it also involves atomic orbitals reordering associated with the Jahn-Teller effect [6,7]. In ferromagnetic Heusler alloys, where the largest strains have been observed, the magnetostrictive effect is closely related to the shape memory effect of the martensitic phase [8,9]. Among the transition/rare-earth intermetallics, Tb$_{0.3}$Dy$_{0.7}$Fe$_2$ (terfenol-D) is the most celebrated example. A unique combination of room temperature giant magnetostriction ($\geqslant 2 \times 10^{-3}$) in a relatively low magnetic field (<1 Tesla) makes this alloy the most widely used material in applications such as sensors and actuators [10]. The magnetostrictive effect in this case is associated with ferromagnetic domains reorientation and is highly dependent on the demagnetized zero-field state, mechanical stress, and actual composition [11,12].

In this work we present another system where notable and strong magnetostructural effects are observed. The intermetallic CeCo$_{1-x}$Fe$_x$Si alloys show antiferromagnetic (AFM) ordering ($T_N = 8.8$ K) in the stoichiometric limit ($x = 0$),

---

[*]Present address: Nuklearmedizinische Klinik und Poliklinik Klinikum rechts der Isar der Technischen Universität, München, Germany.

which weakens as the Fe content is increased [13]. The linear magnetostriction $\Delta L/L$, on the other hand, increases with x approaching a maximum value of $\frac{\Delta L}{L}(16\,\text{T}, 2\,\text{K}) = 3 \times 10^{-3}$ at about the critical concentration $x_c \approx 0.23$ where the magnetic order disappears. Beyond this doping level, the magnetostriction (MS) slowly but steadily decreases again as the system behaves as a heavy fermion. Also at the critical concentration, the MS displays a pronounced and hysteretic jump around $B_m \sim 6$ T, suggestive of a field-induced transition.

Given the subtle interplay between the magnetic order and the Kondo screening, the sharp and large increase of the magnetostriction appears to be associated with the onset of a valence instability around x_c, which gives rise to a small change of the Ce effective valence across B_m. This valence change can also explain the large negative thermal expansion coefficient observed at high fields. The interpretation is supported by the evolution of the unit-cell volume with the Fe content that shows an important Ce volume decrease above $x \sim x_c$ [13]. This is consistent with previous magnetization [14] and x-ray absorption spectroscopy [15] measurements where an important Ce valence change in CeFeSi relative to CeCoSi was reported.

II. RESULTS

High-quality single-phase polycrystalline samples of $CeCo_{1-x}Fe_xSi$ used in this study were prepared by arc melting stoichiometric amounts of the pure elements followed by an annealing procedure as described previously [13]. A high-resolution capacitive dilatometer was used in the dilation experiments, while the magnetization measurements were carried out both in a SQUID magnetometer (up to 5 Tesla) and a VSM magnetometer (up to 14 Tesla). All dilation experiments under magnetic field were performed in the longitudinal configuration, i.e., with the magnetic field B parallel to the sample dimension L being measured. A standard heat-pulse technique was used in the specific heat experiments.

Figure 1 summarizes the main finding of this work. The low-temperature linear forced-magnetostriction (i.e., MS
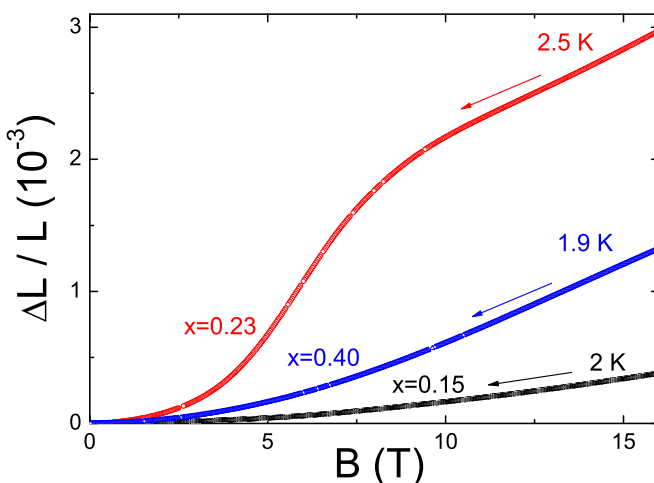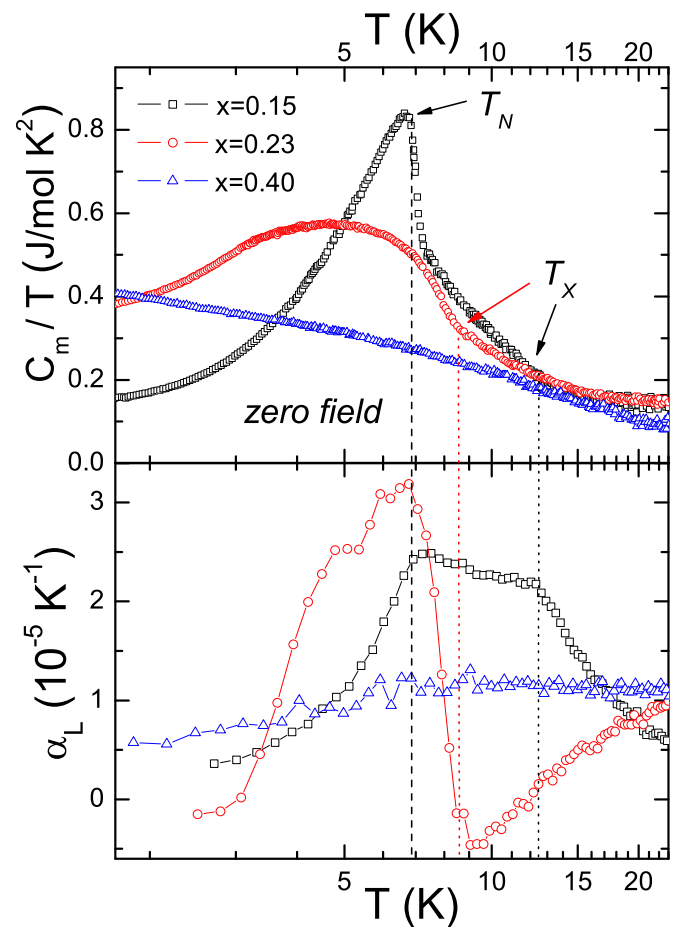
FIG. 2. Top: magnetic contribution to the specific heat divided by temperature at selected Fe doping levels x (adapted from Ref. [13]). The lattice vibrations contribution has been subtracted from the isotypic La compounds. Bottom: linear thermal-expansion coefficient for the same Fe concentrations. Dashed and dotted lines are extrapolations of T_N and T_X from the top to the bottom panel, respectively.

induced by the external field) is shown for three different Fe contents. A very large $\Delta L/L$ is seen at $x = 0.23$ reaching a value as high as 3×10^{-3} at 16 Tesla. The effect is significantly reduced at $x = 0.15$ and $x = 0.4$. As reported in Ref. [13], $x = 0.23$ is approximately the critical concentration x_c at which the antiferromagnetic order vanishes, while $x = 0.15$ is placed well inside the magnetic region ($T_N[x = 0.15] = 6.7$ K) and $x = 0.4$ is nonmagnetic. In this sense, these x values are representative of the different magnetic ground states that are observed.

The top panel of Fig. 2 shows the low-temperature magnetic contribution to the specific heat (C_m/T) for the aforementioned concentrations. As we have shown in previous works [13,16], at low Fe concentrations the magnetic transition at T_N is preceded by a large tail whose onset occurs at T_X ($x = 0.15$ curve). With increasing x, this tail grows up continuously, evolving into a large bump anomaly as the magnetic order collapses around x_c ($x = 0.23$ curve). At higher x, even the bump anomaly disappears ($x = 0.4$ curve).

FIG. 1. Field dependence of the linear magnetostriction at $T \approx 2$ K for different Fe concentrations. Arrows indicate the direction of the field sweeps.

The bottom panel of Fig. 2 shows the corresponding linear thermal-expansion coefficient α_L ($=\alpha_V/3$, the volume thermal-expansion coefficient, given the nontextured nature of the polycrystalline samples) for the selected concentrations. As we pointed out previously [16], the tail in the specific heat at $x = 0.15$ exhibits a remarkably large coupling to the lattice as shown by the double peak structure in α_L, which is consistent with the presence of a structural distortion preceding the magnetic transition, according to a mean-field model [17]. This large spin-lattice coupling is further confirmed by the thermal expansion at $x = 0.23$. While the magnetic order is almost suppressed, α_L shows a broad and large bump (following a pronounced minimum) at basically the same temperature where the bump in the specific heat is observed. Then, at $x = 0.4$, α_L is largely reduced.

An incipient negative expansion is observed at $x = 0.23$. A sign change of the thermal-expansion coefficient has been predicted to occur around a quantum critical point [18]. In this sense, the negative α_L may originate from quantum critical fluctuations becoming dominant as the magnetic order vanishes. The strong non-Fermi liquid behavior observed around x_c [13] backs up this speculation.

Two factors are at play in the suppression of the antiferromagnetic phase as the Fe concentration is increased. On the one hand, there is an increased hybridization of the magnetic moments on the Ce ions f shell with the conduction band, which leads to a screening of the magnetic moments through Kondo physics. On the other hand, since these 111 compounds can be described as a stacking of rare-earth (Ce), transition-metal (Co, Fe), and semimetal (Si) layers [13], the substitution of a transition-metal atom is expected to change the interlayer interaction between the magnetic moments in Ce ions, introducing random links (disorder) in the couplings between planes. A simple double-exchange argument indicates that the nearest-neighbor interlayer magnetic interaction will change sign because Co and Fe differ by a single electron in the d shell. This change in the sign of the interactions is consistent with the magnetic behavior of $GdCo_{1-x}Fe_xSi$ [19–21] and $CeTi_{1-x}Sc_xGe$ [22], where the magnetic order switches from antiferromagnetic to ferromagnetic upon changing x.

Large hysteresis occurs around x_c. This is shown in the top panel of Fig. 3 where three consecutive magnetostriction field-sweeps curves at $T \approx 2$ K are displayed. Curve (i) stands for the first up-sweep after zero-field cooling, while curves (ii) and (iii) are subsequent down-sweep and up-sweep, respectively. This hysteresis is also observed at $x = 0.15$, though smaller [16], and it becomes negligible at $x = 0.4$ (not shown here). It is intriguing that the hysteresis in the magnetization is much smaller, as can be seen in the bottom panel of Fig. 3 where curve labeling follows that of magnetostriction. On the other hand, no hysteresis in the magnetization is observed either at $x = 0.15$ or at $x = 0.4$.

Another interesting aspect to remark is the S shape of the magnetostriction curve at $x = 0.23$ (top panel of Fig. 3). It is suggestive of a field-induced transition as is observed in the relative compound CeTiGe. In this compound, a corresponding pronounced jump in the magnetization (~ 1 μ_B/Ce) at $B_m \approx 12$ T makes it clear that the transition is first order [23]. But in $CeCo_{0.77}Fe_{0.23}Si$, no clear indication of a metamagnetic effect is observed, as seen in the bottom panel of Fig. 3: M
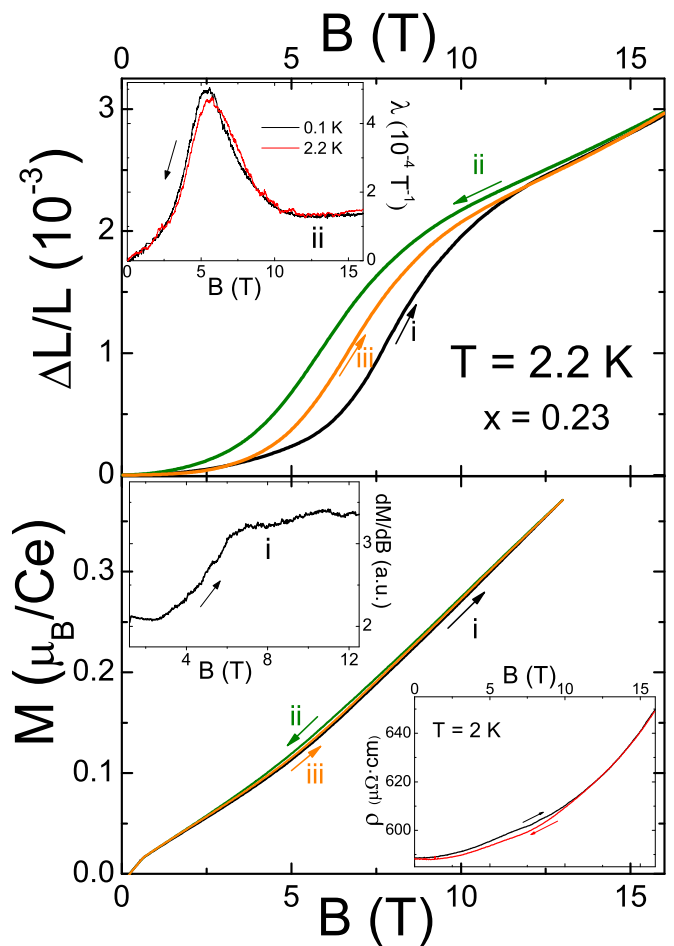

FIG. 3. Top: linear forced-magnetostriction at $T = 2.2$ K; inset: magnetostriction coefficient $\lambda = \frac{\partial \Delta L/L}{\partial B}$ at two different temperatures. Bottom: field dependence of the magnetization at $T = 2.2$ K; left inset: field derivative of the magnetization; right inset: magnetoresistivity at $T = 2$ K. All data corresponds to $x = 0.23 \approx x_c$. See text for details about curves i, ii, iii. Arrows indicate the direction of the field sweeps.

displays just a tiny kink at $B_m \sim 6$ T, where the magnetostriction shows the pronounced increase. Also, magnetoresistance is almost featureless around B_m (right inset in the bottom panel of Fig. 3).

Nonetheless, the longitudinal linear forced magnetostrictions of $CeCo_{0.77}Fe_{0.23}Si$ and CeTiGe show many similarities: (i) the characteristic S-like shape of a metamagnetic transition; (ii) an important hysteresis around B_m; (iii) a very large value $\Delta L(16T)/L \sim 3 \times 10^{-3}$; (iv) a steplike increase $\Delta L/L \sim 2 \times 10^{-3}$ at B_m; (v) temperature independence of $\Delta L/L$ below a few Kelvin (see inset in the top panel of Fig. 3 of this work and Fig. 4 of Ref. [23]).

A clue to understand the large S-shaped magnetostriction in $CeCo_{0.77}Fe_{0.23}Si$ is given by the evolution of the unit-cell volume V_u with the Fe content. $V_u(x)$, which is basically independent of x at low concentrations, shows a noticeable decrease above x_c [13], suggesting that x_c corresponds to the onset of the Ce volume Kondo collapse. This is in agreement with previous magnetization [14] and x-ray absorption spectroscopy [15] measurements, which clearly show that
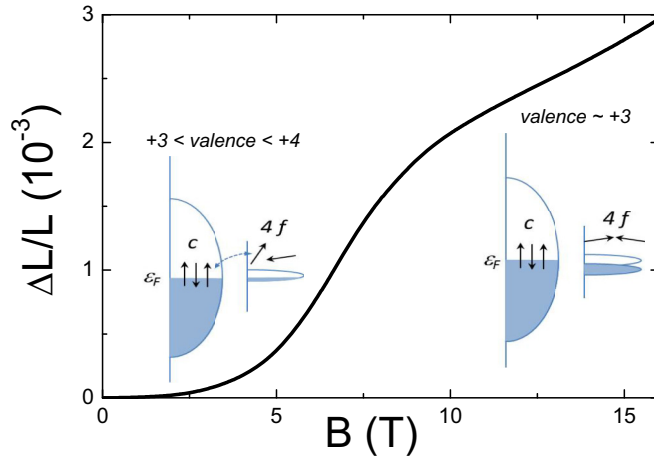
FIG. 4. Schematic picture of the magnetostriction mechanism at the critical concentration. The external magnetic field induces a transition from a Ce intermediate-valence state to a Ce^{3+} predominant state.
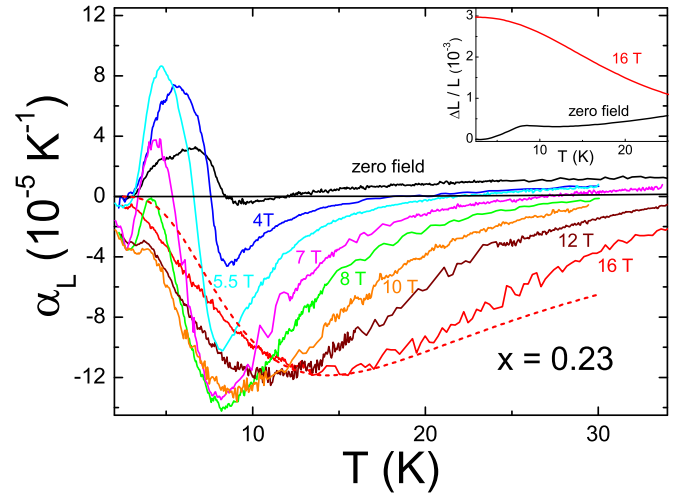

FIG. 5. Linear thermal-expansion coefficient at $x = 0.23$ for different applied magnetic fields. Dotted curve is a fit to the 16 T curve using a doublet model as described in the main text. Inset: $\Delta L(T)/L$ at zero field and 16 T.

Ce^{3+} is the electronic state in CeCoSi, while CeFeSi is in an intermediate valence state.

Hence, the large magnetostriction around x_c seems to be the consequence of an incipient valence instability whose onset is around x_c. At lower Fe concentrations, the $4f$ level is well below the Fermi level ϵ_F and the Ce^{3+} moments are ordered. As x increases, the $4f$ level approaches the Fermi level triggering the hybridization with the conduction band, gradually entering into an intermediate-valence state (a dynamic mixture of Ce^{3+} and Ce^{4+}) and suppressing the magnetic order.

Around x_c the very narrow $4f$ band and ϵ_F are close enough as to start having considerable charge fluctuations. The system is then expected to be particularly susceptible to an external magnetic field. Thus, the incipient nonordered and partially nonlocalized intermediate-valence state can be turned energetically unfavorable under a moderate magnetic field and an ordered (maybe a canted AFM to take advantage of the Zeeman energy), localized 3+ valence state can be reinstated. The large volume difference between the Ce^{4+} and Ce^{3+} configurations explains the large lattice change at B_m.

The situation is depicted schematically in Fig. 4. Indeed, one can estimate a change $\Delta L/L \sim 10^{-3}$ from the evolution of the lattice parameters with x according to Ref. [13] supposing that the lattice volume of CeCoSi is recovered upon the application of a magnetic field (after subtracting the intrinsic expansion considering the analog series $LaCo_{1-x}Fe_xSi$). This should be compared with the jump seen at B_m, which is of the same order. Concomitantly, and though M shows no abrupt change at B_m, its field derivative (i.e., susceptibility) does show a jump at B_m, as observed in the left inset of the bottom panel of Fig. 3.

Figure 5 displays the temperature dependence of the linear thermal expansion coefficient α_L at different applied magnetic fields. Above $B \approx B_m$, α_L shows a characteristic Schottky-like behavior. In fact, the temperature T_m at which α_L is minimum has a linear dependence with the magnetic field above 8 T. Using a doublet model coupled to the magnetic field through

a gyromagnetic factor $g = 3.21$, and assuming the thermal expansion to be proportional to the specific heat, the overall shape of α_L is well fitted for $B > 8$ T (dotted curve in Fig. 5).

The valence change picture offers also a possible explanation for that behavior. Around x_c, the width of the narrow f bands should be order $\sim B_m$. For $B \gtrsim B_m$ one may expect a full split between the spin-up and spin-down bands, with this last one being nearly depopulated. In this intuitive scenario, these two narrow bands can be seen as a two-level system, which gives rise to the Schottky anomaly in α_L. The negative thermal expansion is also consistent with this view: the large MS is suppressed as long as the temperature is increased (see inset of Fig. 5) because the spin-down band is populated and the two-level picture is washed out. Because the hybridization with the conduction band should raise, the Ce ions should slightly lose their 3+ character.

Finally, it is noteworthy to mention that a partial suppression of the hybridization between conduction and $4f$ electrons (i.e., suppression of the Kondo effect with a concomitant effective valence change) by an applied magnetic field has already been reported in $Ce_{0.8}La_{0.1}Th_{0.1}$ [24]. The effect is responsible for the large volume increase at the field-induced reverse transition from the α to the γ phase of Ce.

III. CONCLUSIONS

A strong magnetoelastic effect is reported in the $CeCo_{1-x}Fe_xSi$ alloys. The forced magnetostriction $\Delta L(B)/L$ is shown to change by an order of magnitude in response to slight changes of the Fe content x showing a maximum around the critical concentration x_c where the Néel order is suppressed.

Given the subtle interplay between the magnetic order and the Kondo screening, the large magnetostriction appears to be associated with the onset of a valence instability around x_c. The magnetic field reverses the intermediate-valence state towards a localized 3+ state thus giving rise to a large volume change. This interpretation is supported by the evolution of

the unit-cell volume with x, which confirms an important Ce volume reduction [13], in agreement with magnetization [14] and x-ray absorption spectroscopy [15] measurements that show a considerable Ce valence change between CeCoSi and CeFeSi. The Schottky-like shape shown by the large and negative thermal-expansion coefficient at high field is also consistent with this Kondo collapse/valence change scenario.

At x_c, the magnetostriction also shows an important hysteresis, which is almost absent in the magnetization. This would imply a strong pinning mechanism acting on the atomic lattice but not on the magnetic moments.

The magnetostrictive effect maximum strength around x_c is something we could have anticipated given the close competition between different energy scales. Indeed, it has been predicted and demonstrated in $CeRu_2Si_2$ (the paradigmatic example of a Kondo metamagnetic system in the very border of a magnetic instability [25]) upon small substitutions of Ce by La [26] or Ru by Rh [27]. However, the effect is not as evident as in $CeCo_{1-x}Fe_xSi$.

[1] P. Fazekas, *Lecture Notes on Electron Correlation and Magnetism* (World Scientific, Singapore, 2003).

[2] N. P. Grazhdankina, Sov. Phys. Usp. **11**, 727 (1969).

[3] M. Ekman, B. Sadigh, K. Einarsdotter, and P. Blaha, Phys. Rev. B **58**, 5296 (1998).

[4] M. R. Ibarra, P. A. Algarabel, C. Marquina, J. Blasco, and J. García, Phys. Rev. Lett. **75**, 3541 (1995).

[5] V. F. Correa, N. Haberkorn, G. Nieva, D. J. García, and B. Alascio, Europhys. Lett. **98**, 37003 (2012).

[6] A. J. Millis, P. B. Littlewood, and B. I. Shraiman, Phys. Rev. Lett. **74**, 5144 (1995).

[7] T. Kimura, Y. Tomioka, A. Asamitsu, and Y. Tokura, Phys. Rev. Lett. **81**, 5920 (1998).

[8] O. Söderberg, A. Sozinov, Y. Ge, S.-P. Hannula, and V. K. Lindroos, *Handbook of Magnetic Materials* (Elsevier B. V., Amsterdam, 2006), Vol. 16, pp. 139.

[9] T. Sakon, N. Fujimoto, T. Kanomata, and Y. Adachi, Metals **7**, 410 (2017).

[10] F. Claeyssen, N. Lhermet, R. Le Letty, and P. Bouchilloux, J. Alloys Compd. **258**, 61 (1997).

[11] D. C. Jiles and J. B. Thoelke, Phys. Status Solidi A **147**, 535 (1995).

[12] X. Gao, Y. Pei, and D. Fang, Acta Mech. Solida Sin. **21**, 15 (2008).

[13] J. G. Sereni, M. Gómez Berisso, D. Betancourth, V. F. Correa, N. Caroca Canales, and C. Geibel, Phys. Rev. B **89**, 035107 (2014).

[14] R. Welter, G. Venturini, and B. Malaman, J. Alloys Compd. **189**, 49 (1992).

[15] O. Isnard, S. Miraglia, R. Welter, and B. Malaman, J. Synchrotron Radiat. **6**, 701 (1999).

[16] V. F. Correa, D. Betancourth, J. G. Sereni, N. Caroca Canales, and C. Geibel, J. Phys.: Condens. Matter **28**, 346003 (2016).

[17] W. G. Carreras Oropesa, V. F. Correa, J. G. Sereni, D. J. García, and P. S. Cornaglia, J. Phys.: Condens. Matter **30**, 295803 (2018).

[18] M. Garst and A. Rosch, Phys. Rev. B **72**, 205129 (2005).

[19] S. A. Nikitin, T. I. Ivanova, I. G. Makhro, and Yu. A. Tskhadadze, J. Magn. Magn. Mater. **157-158**, 387 (1996).

[20] P. Wlodarczyk, L. Hawelek, P. Zackiewicz, T. Rebeda Roy, A. Chrobak, M. Kaminska, A. Kolano-Burian, and J. Szade, Mater. Chem. Phys. **162**, 273 (2015).

[21] V. Vildosola *et al.*, (unpublished).

[22] J. G. Sereni, P. Pedrazzini, M. Gómez Berisso, A. Chacoma, S. Encina, T. Gruner, N. Caroca-Canales, and C. Geibel, Phys. Rev. B **91**, 174408 (2015).

[23] M. Deppe, S. Lausberg, F. Weickert, M. Brando, Y. Skourski, N. Caroca-Canales, C. Geibel, and F. Steglich, Phys. Rev. B **85**, 060401(R) (2012).

[24] F. Drymiotis, J. Singleton, N. Harrison, J. C. Lashley, A. Bangura, C. H. Mielke, L. Balicas, Z. Fisk, A. Migliori, and J. L. Smith, J. Phys.: Condens. Matter **17**, L77 (2005).

[25] L. Puech, J. M. Mignot, P. Lejay, P. Haen, J. Flouquet, and J. Voiron, J. Low Temp. Phys. **70**, 237 (1988).

[26] A. Lacerda, A. de Visser, L. Puech, P. Lejay, and P. Haen, J. Magn. Magn. Mater. **76-77**, 138 (1988).

[27] T. Takeuchi and Y. Mikayo, J. Phys. Soc. Jpn. **65**, 3242 (1996).